A On-Site Testing Method to Verify The Assumption of Rigid Floor in Urban Construction

Yu Chen*

Department of Mechanical Engineering, HKU, HongKong, 999077, China

*Corresponding author's e-mail: chen_yu1109@163.com

Abstract. Due to the increasing complexity of building functions and diversity of shapes, structures are becoming more and more complex. This article will use on-site testing methods to verify whether the urban building floor meets the assumption of a rigid floor. Firstly, a mathematical relationship formula is established to validate the rigid floor assumption, and multiple measurement points in the X and Y directions of the same test floor are measured using sensors at medium and small speeds respectively, and the obtained data is inputted into the mathematical relationship formula to verify the rigid floor assumption. The results show that under natural excitation, this test floor meets the assumption of a rigid floor and there is no continuous non-rigid movement. The relative error measured at a small speed is better than that measured at a medium speed, and it is more suitable for measuring the floor velocity.

Keywords: On-site testing methods; mathematical relationship; rigid floor assumption.

1 Introduction

In order to meet the needs of engineering design, designers are looking for reasonable methods to assume the stiffness of floors [1]. In order to simplify calculations, the floor is usually assumed to be a rigid floor in the analysis and design of building structures, and on this basis, the stiffness center of the floor is determined to determine the structural stress under lateral loads (such as wind loads and earthquake effects).

The assumption of a rigid floor assumes that the rigidity of the floor in the plane is infinitely large. This means that the distance between any two points in the horizontal plane of the floor does not change during the process of loading and deformation [2].

Assuming a rigid floor makes it possible to express the displacement of all positions on the floor in its centroid plane [3]. This method significantly reduces the calculation degree of freedom of the building structure, improves numerical solving efficiency, simplifies the calculation method, and in most cases, the deviation between assuming an infinitely rigid floor and the actual situation is small and acceptable from an engineering perspective.

However, there are also some potential problems in the assumption of rigid floor slab [4]. Because ignoring the importance of the wing edge of the floor beam on the

Z. Ahmad et al. (eds.), *Proceedings of the 2024 5th International Conference on Urban Construction and Management Engineering (ICUCME 2024)*, Advances in Engineering Research 242,
https://doi.org/10.2991/978-94-6463-516-4_9

total strength of the components, the total stiffness of the structure is small and the cycle is easy to lengthen, thus bringing hidden dangers to the building safety [5]. The safety problem in urban construction is difficult to find through theoretical analysis, but it can be effectively detected by the field measurement method.

Through the summary of the literature, it is found that there are few studies on the rigid floor hypothesis in the current literature, and mainly focus on theoretical analysis, and there is a lack of research on exploring the rigid floor assumption through the field measurement method [6]. This paper will test the actual floor in the urban building to make up the relevant literature vacancy.

2 Theoretical Analysis

The actual floor of urban buildings will be verified by the basic concept of rigid floor assumption [7]. During the motion of the floor, there can be both translational and rotational movements, and the actual rigid body displacement is the composition of the translational displacement and rotational displacement. To analyze the floor, we can start from any point on the floor that is not the center of rotation and first analyze its rotational motion [8].

As shown in Figure 1, the coordinates of point A $(x_A, y_A)$and O (x_O, y_O), the distance between point O and point A is ρ, and the Angle between line segment OA and the X-axis is α. If point A rotates from point O at A small Angle θ to point A', the vertical line from point A' to line segment OA intersects OA at pointA'', because Angle θ is a small Angle, Then the displacement of point A in the Y-axis direction can be replaced by Y_A [9].

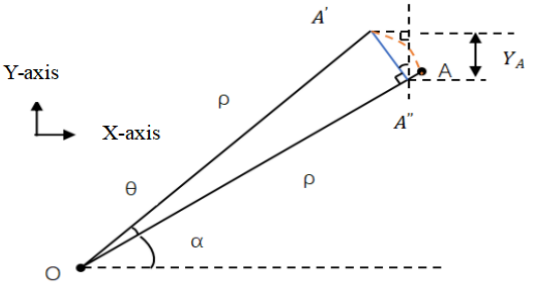

Fig. 1. Rotation diagram of any point A on the floor.

$$\rho=\sqrt{(x_A-x_O)^2+(y_A-y_O)^2} \tag{1}$$

Arc $AA'=\rho\theta$, line segment $A'A''=\rho\tan\theta$. Since θ is a small Angle,$\rho\theta=\rho\tan\theta$, the arc AA'can be approximated by the line segment$A'A''$.

$$\cos\alpha=\frac{x_A-x_O}{\rho} \tag{2}$$

Because θ is a small Angle,

$$Y_A=\rho\theta\cos\alpha=\theta(x_A-x_O) \tag{3}$$

$$X_A=\rho\theta\sin\alpha=\theta(y_A-y_O) \tag{4}$$

The total displacement of a point on the floor in the Y-axis direction is ΔY, the displacement generated by rotation in the Y axis direction is Δy, and the displacement generated by translation in the Y axis direction is Δy_0.

$$\Delta y=\rho\theta\cos\alpha=\theta(x-x_0) \tag{5}$$

$$\Delta Y=\Delta y+\Delta y_0) \tag{6}$$

Take the time derivative of the above formula,

$$V_y=v_y+v_{0y}=w(x-x_0)+v_{0y} \tag{7}$$

V_y is the total instantaneous velocity of a point on the floor in the Y-axis direction; v_y is the instantaneous velocity of rotation in the Y-axis direction; v_{0y} is the instantaneous velocity of translation in the Y-axis direction; w is the instantaneous angular velocity during rotation [10].

By the same token, the total instantaneous velocity in the X-axis is V_x,

$$V_x=v_x+v_{0x}=w(y-y_0)+v_{0x} \tag{8}$$

The four corner points on the edge of the rectangular floor are taken as points 1, 2, 3 and 4, and their coordinates are respectively points $1(x_1,y_1)$, $2(x_2,y_2)$, $3(x_3,y_3)$and $4(x_4,y_4)$, as shown in Figure 2.

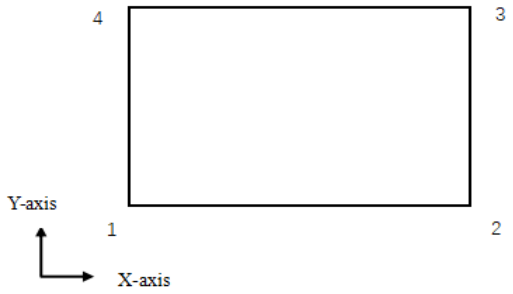

Fig. 2. Diagram of the first method.

O point as the center of rotation and the position of the unknown of the floor slab, according to the above formula can get on the floor of the four corner respectively on the X axis and Y axis of the instantaneous velocity $V_{1y},V_{2y},V_{3y},V_{4y},V_{1x},V_{2x},V_{3x},V_{4x}$.

$$V_{1y}=w(x_1-x_O)+v_{Oy} \tag{9}$$

$$V_{2y}=w(x_2-x_O)+v_{Oy} \tag{10}$$

$$V_{3y}=w(x_3-x_O)+v_{Oy}) \tag{11}$$

$$V_{4y}=w(x_4-x_O)+v_{Oy} \tag{12}$$

$$V_{1x}=w(y_1-y_O)+v_{Ox} \tag{13}$$

$$V_{2x}=w(y_2-y_O)+v_{Ox} \tag{14}$$

$$V_{3x}=w(y_3-y_O)+v_{Ox} \tag{15}$$

$$V_{4x}=w(y_4-y_O)+v_{Ox} \tag{16}$$

Because $x_1 = x_4, x_3 = x_2, y_1 = y_2, y_4 = y_3$,so $V_{1x} = V_{2x}, V_{3x} = V_{4x}, V_{1y} = V_{4y}, V_{2y} = V_{3y}$.

According to the above formula can be simply measured four floor slab edge Angle points in X axis and Y axis at the same time the instantaneous velocity of $V_{1y}, V_{2y}, V_{3y}, V_{4y}, V_{1x}, V_{2x}, V_{3x}, V_{4x}$ and compare, if $V_{1x} = V_{2x}, V_{3x} = V_{4x}, V_{1y} = V_{4y}, V_{2y} = V_{3y}$,it can be concluded that $x_1 = x_4, x_3 = x_2, y_1 = y_2, y_4 = y_3$.these formulas show floor in the process of translation and rotation of the tiny movement did not happen any relative displacement, so to prove that the rigid floor 4 floor is not happen any deformation [11].

3 Test Scheme

During the actual testing, the 941B type ultra-low frequency accelerometer was used, which has the following characteristics: micro toggle switch, capable of directly measuring acceleration or velocity response, high resolution, easy to operate, and can be connected to a dynamic data collector through a data cable [12]. The pick-up sensor has four gear positions, with large, medium, small velocity and acceleration gears.

Table 1 lists the main technical specifications of the speed gear of the horizontal vibration pickup used in the test:

Table 1. B Speed profile technical specifications of the vibration pickup.

Technical index	Small speed	Medium speed	High speed
sensitivity（v*s/m)	23	2.4	0.8
Maximum range（m/s)	0.125	0.3	0.6
Resolution（m/s)	4×10-8	4×10-7	1.6×10-6

Due to the small sensitivity of large speed, the test results may not be accurate, so this study only carried out the measurement of medium speed and small speed [13].

The object measured in this paper is the conference room of the School of Civil Engineering and Architecture of our school, as shown in Figure 3.

Fig. 3. Field diagram of the floor measured.

Install speed sensors around the test floor. Figure 4 shows the sensor positions.

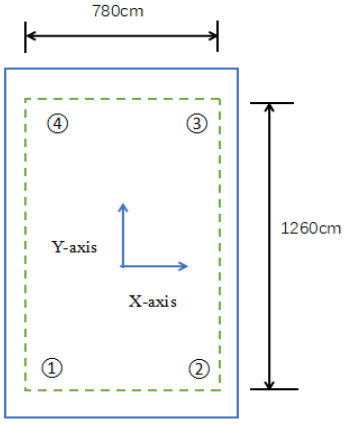

Fig. 4. Layout of speed sensors.

4 Verification of Rigid Floor Assumptions

Verify that $V_{1x} = V_{2x}, V_{3x} = V_{4x}, V_{1y} = V_{4y}, V_{2y} = V_{3y}$, you can only compare the x direction formula, that is $V_{1x} = V_{2x}, V_{3x} = V_{4x}$, you can prove that the floor does rigid movement.In order to verify whether the above formula is correct, the small velocity in X direction and the instantaneous velocity at the same time of the medium velocity in the experimental data are compared [14].

4.1 Working Condition 1 Verification of V1X=V2X

4.1.1. Medium Speed Gear Measurement

To verify that $V_{1x} = V_{2x}$, first use the direct method, that is, verify that V_{1x}/V_{2x}=1.The relative error is obtained by comparing the value of V_{1x}/V_{2x} obtained after processing with 1 [15]. Select the first 7000 data points and explore the relative error of each point of the first 7000 data points [16]. If the data point exceeds the 95% confidence range of the normal distribution, it is considered to be an anomaly.

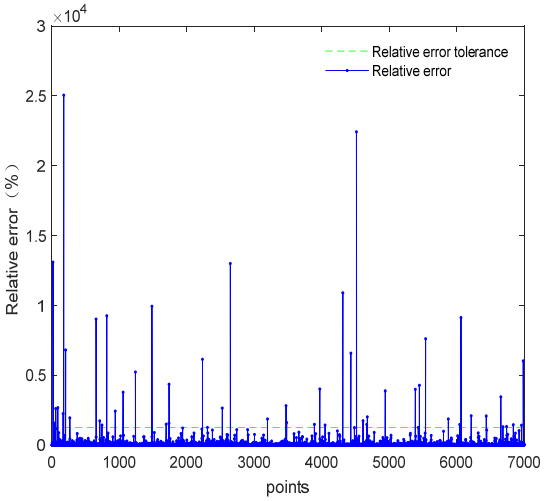

Fig. 5. Relative errors of V_{1x} and V_{2x} at dense access points (medium speed).

As shown in Figure 5, a large number of anomalies are found. At this time, 20 points near the anomalies are investigated, and it is found that the anomalies all belong to one point and belong to noise interference, rather than the non-rigid movement of the floor [17].

4.1.2 Small Speed Gear Measurement

Select the first 7000 data points and explore the relative error of each point of the first 7000 data points. If the data point exceeds the 95% confidence range of the normal distribution, it is considered to be an anomaly.

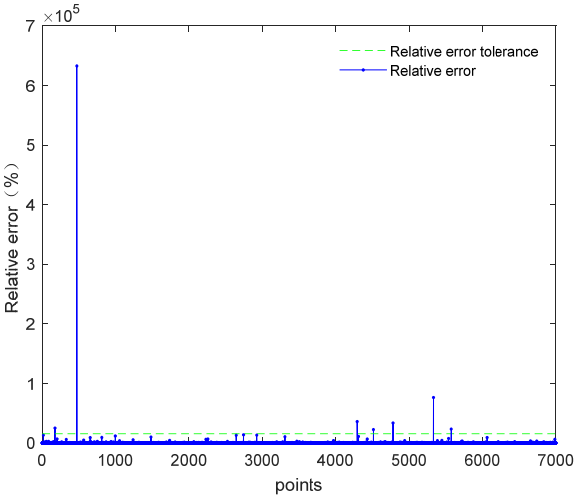

Fig. 6. Relative error of V_{1x} and V_{2x} at dense access points (small speed).

As shown in Figure 6, it is found that 473, 4293, 4781, 5332 and 5574 are abnormal points, and the relative errors are 632500%, 35920%, 33540%, 76310% and 55740% respectively. The abnormal points belong to a point, and it is inferred that the floor is affected by noise interference, and it is not a non-rigid movement of the floor.

4.1.3 Comparison Between Medium Speed Gear and Small Speed Gear

If the slope is used to calculate the relative error, that is, the slope method, check the formula $\frac{X_2V_3-X_1V_3}{X_2-X_1} / \frac{X_2V_4-X_1V_4}{X_2-X_1}$=1.The mean relative error and outlier rate of each group were compared by direct method and slope method respectively [18].

Table 2. Comparison of medium speed and small speed (direct method).

	method	Mean relative error(%)	Outlier rate(%)
Medium speed	Direct method	11.24	14.42
Small speed		11.69	14.22

As shown in Table 2, comparing the data of medium speed and small speed measured by the direct method, it can be seen that the mean relative error of medium speed is slightly smaller than that of small speed, and the anomaly rate is 0.20% higher.

Table 3. Comparison of medium speed and small speed (slope method).

	method	Mean relative error(%)	Outlier rate(%)
Medium speed	Slope method	10.50	14.64
Small speed		10.82	14.03

As shown in Table 3, the data measured by the slope method at medium speed and small speed are compared. The mean relative error of medium speed is not much different from that of small speed, and the speed with small anomaly rate is 0.61% higher [19].

Comparing the data obtained by the direct method and the slope method, it can be seen that the mean relative error of the slope method is smaller, while the direct outlier rate method and the slope method have little difference.

4.2 Working Condition 2 Verification of V3X=V4X

4.2.1 Medium Speed Gear Measurement

Select the first 7000 data points, explore the relative error of each point of the first 7000 data points, and data points that exceed the 95% confidence range of the normal distribution are considered as abnormal points.

As shown in Figure 7, 2067, 2339, 3904, 5208, 6139, and 6180 are found to be anomalies, and the phase alignment errors are 12110%, 8524%, 307600%, 8026%, 7751%, and 12720%, respectively [20]. The abnormal points all belong to one point, and the floor is not in non-rigid movement.

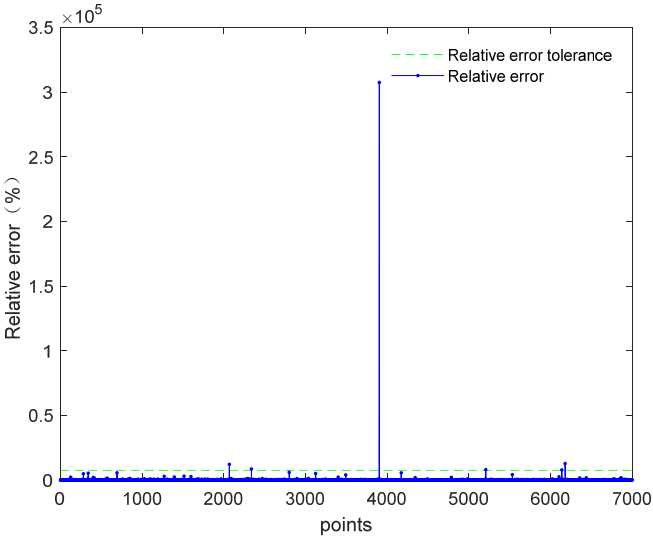

Fig. 7. V_{3x} and V_{4x} relative errors at dense access points (medium speed).

4.2.2 Small Speed Gear Measurement

Imported V_{3x} and V_{4x} data at small speed into Matlab, selected the first 7000 data points, explored the relative error of each point of the first 7000 data points, and data points exceeding the 95% confidence range of normal distribution were considered as abnormal points [21].

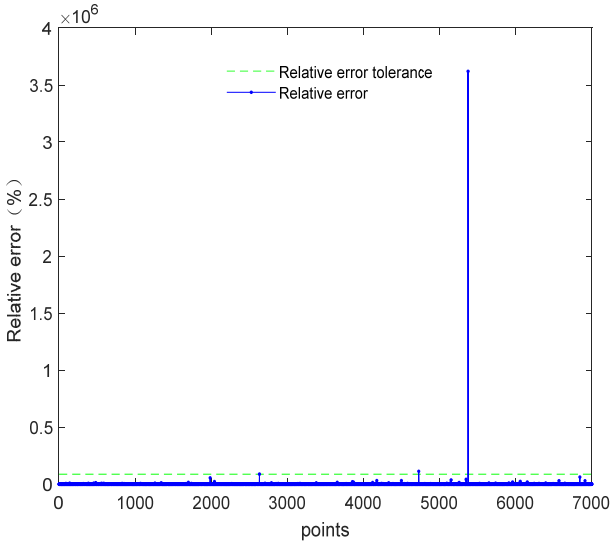

Fig. 8. V_{3x} and V_{4x} relative errors at dense access points (small speed).

As shown in Figure 8, 2633, 4726 and 5374 are abnormal points, and the relative errors are 88460%, 112700% and 3619000% respectively. After probing the abnormal points, it is found that they all belong to one point and belong to noise interference, rather than non-rigid movement of the floor.

4.2.3 Comparison Between Medium Speed Gear and Small Speed Gear

The relative errors at medium speed and small speed are compared respectively.

Table 4. Comparison of medium speed and small speed (direct method).

	method	Mean relative error(%)	Outlier rate(%)_
Medium speed	Direct method	6.90	14.82
Small speed		5.05	14.67

It can be seen from Table 4 that the mean relative error of small speed is smaller, and the anomaly rate is 0.15% smaller than that of medium speed.

Table 5. Comparison of medium speed and small speed (slope method).

	method	Mean relative error(%)	Outlier rate(%)
Medium speed	Slope method	6.33	15.38
Small speed		4.54	14.70

As shown in Table 5, comparing the data of medium speed and small speed measured by slope method, it can be seen that the mean relative error of small speed is better than that of medium speed, and the anomaly rate is 0.68% lower.

Comparing the data obtained by the direct method and the slope method, it can be seen that compared with the direct method, the average relative error of each group using the slope method is smaller.

5 Conclusions

1) In engineering terms, the test floor selected in this article can meet the assumption of rigid motion in 85% of cases under natural excitations.

2) The relative error of measuring a rigid floor using small speed is better than medium speed. Small speed has a better signal-to-noise ratio and is more suitable for measuring floor velocity.

3) By exploring the abnormal points, it was found that there was no continuous non-rigid motion in the test floor during this test.

4) The data processing method of slope can eliminate the accumulation error of noise and reflect the rigid motion of the floor more accurately.

5) In the test part of this paper, the placement of sensors in X and Y directions can not ensure that the direction is completely correct. And there will be angle deviation, which leads to the error of data.

6) This paper only analyzes a piece of building floor panels, without deeply considering the analysis results of different types of floor panels, so a more complete test scheme should be developed for further analysis.

References

1. Batalha, N., Rodrigues, H., Sousa, R., Varum, H.(2022) Seismic assessment of existing precast RC industrial buildings in Portugal. Structures, 41: 777-786.
2. Ruggieri, S., Porco, F., Uva, G. (2018)A numerical procedure for modeling the floor deformability in seismic analysis of existing RC buildings. Journal of Building Engineering, 19: 273-284.
3. Sivori, D., Lepidi, M., Cattari, S. (2020)Ambient vibration tools to validate the rigid diaphragm assumption in the seismic assessment of buildings.Earthquake Engineering & Structural Dynamics, 49(2): 194-211.
4. Hadianfard, M. A., Sedaghat, S. (2013)Investigation of joist floor diaphragm flexibility on inelastic behavior of steel braced structures. Scientia Iranica Transaction A-Civil Engineering, 20(3): 445-453.
5. Karampour, H., Piran, F., Faircloth, A., Talebian, N., Miller, D., (2023)Vibration of Timber and Hybrid Floors: A Review of Methods of Measurement, Analysis, and Design, Buildings, 13, 1756.
6. Chen, W., Wang, J. (2018)Explain the influence of rigid floor assumption on large hole structure. Southern Energy Construction, 5 (A01): 150-156.
7. Zhang, Y., Luo,Y., Guo, X., Li, Y., Huang, Q. (2021) A new seismic damage assessment method for single-layer steel latticed shells considering multi-modal contribution, Structures, 33: 4670-4689.
8. Yang, Y., Huang, J. P. (2021)Analysis of the influence of thickness change on the deformation of floor of a frame. Guangdong Building Materials, 037 (10): 63-64.
9. Vassiliou, M. F., Mackie, K. R. (2014)Dynamic response analysis of solitary flexible rocking bodies: Modeling and behavior under pulse-like ground excitation. Earthquake Engineering and Structural Dynamics, 43(10): 1463-1481.
10. Tulebekova, S., Malo, K. A., Rønnquist, A., Nåvik, P. (2022)Modeling stiffness of connections and non-structural elements for dynamic response of taller glulam timber frame buildings. Engineering Structures, 261: 114209.
11. Aloisio, A., Pasca, D., Tomasi, R., Fragiacomo, M. (2020)Dynamic identification and model updating of an eight-storey CLT building. Engineering Structures, 213: 110593.
12. Larsson, C., Abdeljaber, O., Bolmsvik, Å., Dorn, M. (2022)Long-term analysis of the environmental effects on the global dynamic properties of a hybrid timber-concrete building. Engineering Structures, 268: 114726.
13. Kurent, B., Brank, B., Ao, W. K. (2023)Model updating of seven-storey cross-laminated timber building designed on frequency-response-functions-based model testing. Struct Infrastruct Eng ;19(2):178-196.
14.]Jaimes, M. A., Chávez, M. M., Peña, F., García, A.D. (2021)Out-of-plane mechanism in the seismic risk of masonry façades. Bulletin of Earthquake Engineering, 19(3): 1509-1535.
15. Di, S. L., Magliulo, G., Angela, D., Cosenza, E. (2019)Experimental assessment of the seismic performance of hospital cabinets using shake table testing. Earthquake Engineering and Structural Dynamics, 48(1): 103-123.
16. Fragiadakis, M., Diamantopoulos, S., (2020)Fragility and risk assessment of freestanding building contents. Earthquake Engineering and Structural Dynamics, 49(10): 1028-1048.
17. Rashid. M., Dhakal, R.P., Sullivan, T. J. (2021). Seismic design of acceleration-sensitive non-structural elements in New Zealand: State-of-practice and recommended changes. Bulletin of the New Zealand Society for Earthquake Engineering, 54(4): 243-262.
18. Angela, D., Magliulo, G., Cosenza, E. (2021)Towards a reliable seismic assessment of rocking components. Engineering Structures, 230: 111673.

19. Haymes, K., Sullivan, T., Chandramohan, R. (2020)A practice-oriented method for estimating elastic floor response spectra". Bulletin of the New Zealand Society for Earthquake Engineering, 53(3): 116-136.
20. Ao, W. K., Pavic, A., Kurent, B., Perez, F. (2023)Novel FRF-based fast modal testing of multistorey CLT building in operation using wirelessly synchronised data loggers. J Sound Vib, 548: 117551.
21. Blaž, K., Wai, K. A., Aleksandar, P., Fernando, P., Boštjan, B., (2023)Modal testing and finite element model updating of full-scale hybrid timber-concrete building,Engineering Structures, 289: 116250.